The Journal of Nutrition
Ingestive Behavior and Neurosciences

Iron Is Essential for Neuron Development and Memory Function in Mouse Hippocampus[1–3]

Erik S. Carlson,[4–7] Ivan Tkac,[8] Rhamy Magid,[6] Michael B. O'Connor,[9,10] Nancy C. Andrews,[11] Timothy Schallert,[10,11] Hiromi Gunshin,[14,15] Michael K. Georgieff,[5–7]* and Anna Petryk[6,9]

[4]Medical Scientist Training Program, [5]Graduate Program in Neuroscience, [6]Pediatrics, [7]Center for Neurobehavioral Development, [8]Center for Magnetic Resonance Research, and [9]Genetics, Cell Biology and Development, University of Minnesota Medical School, Minneapolis, MN 55455; [10]Howard Hughes Medical Institute, Chevy Chase, MD 20815; [11]Duke University School of Medicine, Durham, NC 27710; [12]Institute for Neuroscience, and [13]Department of Psychology, University of Texas, Austin, TX 78712; and [14]Department of Nutrition, University of Massachusetts, Amherst, MA 01003

Abstract

Iron deficiency (ID) is the most prevalent micronutrient deficiency in the world and it affects neurobehavioral outcome. It is unclear whether the effect of dietary ID on the brain is due to the lack of neuronal iron or from other processes occurring in conjunction with ID (e.g. hypoxia due to anemia). We delineated the role of murine *Slc11a2* [divalent metal ion transporter-1 (DMT-1)] in hippocampal neuronal iron uptake during development and memory formation. *Camk2a* gene promoter-driven cre recombinase (Cre) transgene (*Camk2a-Cre*) mice were mated with *Slc11a2 flox/flox* mice to obtain nonanemic *Slc11a2*$^{hipp/hipp}$ (double mutant, hippocampal neuron-specific knockout of Slc11a2$_{hipp/hipp}$) mice, the first conditionally targeted model of iron uptake in the brain. *Slc11a2*$^{hipp/hipp}$ mice had lower hippocampal iron content; altered developmental expression of genes involved in iron homeostasis, energy metabolism, and dendrite morphogenesis; reductions in markers for energy metabolism and glutamatergic neurotransmission on magnetic resonance spectroscopy; and altered pyramidal neuron dendrite morphology in area 1 of Ammon's Horn in the hippocampus. *Slc11a2*$^{hipp/hipp}$ mice did not reach the criterion on a difficult spatial navigation test but were able to learn a spatial navigation task on an easier version of the Morris water maze (MWM). Learning of the visual cued task did not differ between the *Slc11a2*$^{WT/WT}$ and *Slc11a2*$^{hipp/hipp}$ mice. *Slc11a2*$^{WT/WT}$ mice had upregulation of genes involved in iron uptake and metabolism in response to MWM training, and *Slc11a2*$^{hipp/hipp}$ mice had differential expression of these genes compared with *Slc11a2*$^{WT/WT}$ mice. Neuronal iron uptake by DMT-1 is essential for normal hippocampal neuronal development and *Slc11a2* expression is induced by spatial memory training. Deletion of *Slc11a2* disrupts hippocampal neuronal development and spatial memory behavior. J. Nutr. 139: 672–679, 2009.

Introduction

Proper iron balance in the brain appears to be essential for normal cognitive development and function. However, previous studies on the effects of early iron deficiency (ID)[16] on the developing brain have relied on dietary or genetic (e.g. Belgrade rat, *microcytic anemia* mouse, or H-ferritin knockout mice) models that induce total body ID and ID anemia (IDA) in the mother and offspring. Elucidating the specific role of iron in the development of particular brain cell types or structures has not been possible through these models because of concomitant, potentially neuropathological processes such as anemia, tissue hypoxia, stress, and increased uptake of other divalent metals.

[1] Supported by the grants: NIH: R21 HD054490, R01 HD 29421, Minnesota Medical Foundation at the University of Minnesota, and the Vikings Children's Fund at the University of Minnesota to M.K.G.; NIH: R01 DK53813 and R01 HL51057 to N.C.A.; NIH: NINDS Individual Kirschstein-NRSA F31-NS047876, a seed grant from the American Medical Association Foundation, and the Dr. Warren J. Warwick and Henrietta Holm Warwick Fellowship Award to E.S.C.
[2] Author disclosures: E. S. Carlson, I. Tkac, R. Magid, M. B. O'Connor, N. C. Andrews, T. Schallert, H. Gunshin, M. K. Georgieff, and Anna Petryk, no conflicts of interest.
[3] Supplemental Figures 1–5, Supplemental Methods, and Supplemental Table 1 are available with the online posting of this paper at jn.nutrition.org.
[15] Deceased.
* To whom correspondence should be addressed. E-mail: georg001@umn.edu.

[16] Abbreviations used: CA1, Cornus Ammon 1 (area 1 of Ammon's Horn in hippocampus); *Camk2a-Cre*, *Camk2a* gene promoter-driven cre recombinase transgene; Cre, cre recombinase; DMT1, divalent metal ion transporter-1; ID, iron deficiency; IDA, iron deficiency anemia; MWM, Morris water maze; MRS, magnetic resonance spectroscopy; P, postnatal day; qPCR, quantitative PCR; *Slc11a2*$^{hipp/hipp}$, homozygous hippocampal pyramidal neuron-specific (cre recombinase-mediated, *flox/flox Slc11a2*) *Slc11a2* knockout mice; *Slc11a2*$^{WT/WT}$, wild-type (cre recombinase-negative, *flox/flox Slc11a2*) littermates of *Slc11a2*$^{hipp/hipp}$ mice; Tf, diferric transferrin; TfR1, Transferrin Receptor-1; VOI, volume of interest.

Manuscript received August 26, 2008. Initial review completed October 21, 2008. Revision accepted January 13, 2009.
First published online February 11, 2009; doi:10.3945/jn.108.096354.

In this study, we presented a mouse model that specifically addresses the role of iron in the developing hippocampus not only to avoid confounding processes, but also to examine the contribution of ID-induced hippocampal dysfunction to the overall clinical spectrum of abnormal cognitive behavior in early IDA (1).

Early IDA alters recognition memory behavior in humans (2,3) and rodents (4–8) in several hippocampus-dependent tasks. IDA leads to molecular, metabolic, structural, and synaptic changes in the hippocampus that accompany behavioral changes, which remain even after iron repletion (9,10). The alterations in pre- and postsynaptic plasticity in the hippocampus provide a link between cellular changes in the hippocampus and memory deficits in ID rats (11).

Neurons accrete iron by a classical cellular uptake mechanism. Diferric transferrin (Tf) is synthesized and secreted by oligodendrocytes and astrocytes, localizes to the extracellular fluid space, and binds Transferrin Receptor-1 (TfR1) expressed on the neuronal cell membrane (12,13). The TfR1-Tf complex is taken up by a clathrin-coated endosome. Iron molecules are off-loaded in their ferrous state and transported across the endosomal membrane by Slc11a2 [divalent metal ion transporter-1 (DMT-1)] (14). The system is appropriately regulated by neuronal iron status in vivo (15) and is activated and inhibited by excitatory and inhibitory neurotransmitters, respectively, in vitro (16).

The conditionally targeted *Slc11a2* knockout mouse model is the first, to our knowledge, to isolate the effect of ID without anemia in hippocampal neurons in vivo. In this study, we demonstrated that the lack of iron alone is responsible for molecular, biochemical, structural, and behavioral abnormalities in IDA and also showed that memory training induces markers of neuronal iron uptake in *Slc11a2*$^{WT/WT}$ mice.

Methods

Mice. All experiments were approved by the Institutional Animal Care and Use Committee of the University of Minnesota and performed in accordance with the NRC's Guide for the Care and Use of Laboratory Mice. Targeted *Slc11a2 flox/flox* mice in a 129 J1 background strain (17) were crossed with mice expressing a *Camk2a* gene promoter-driven cre recombinase (Cre) transgene (CaMKIIα-*Cre*) [L7ag#13 line (18)] transgenic mice in a C57BL/6J background to generate a double mutant, hippocampal neuron-specific knockout of *Slc11a2* (*Slc11a2*$^{hipp/hipp}$ mice) in a mixed, Filial 2 generation, 129 J1/C57BL/6J background. All experiments except dendrite apical shaft measurements were performed in littermates of this mixed background strain. To visualize neurons for dendrite measurements, *Slc11a2*$^{hipp/hipp}$ mice were backcrossed over 6 generations into C57BL/6J and then crossed with Tg(*Thy1-YFP*)23Jrs mice in a C57BL/6J background (19) obtained from the Jackson Laboratory to generate triple mutants with central nervous system neurons randomly labeled with yellow fluorescent protein (Supplemental Methods).

Hematocrit measurement. Blood samples for measuring hematocrit were taken from postnatal d (P) 90 *Slc11a2*$^{hipp/hipp}$ mice ($n = 9$) and wild-type littermates (*Slc11a2*$^{WT/WT}$ mice) ($n = 22$) with heparinized capillary tubes from the right cardiac atrium before the mice were perfused. Tubes were centrifuged at 3000 $\times$ *g*; 20 min and measured with a standard hematocrit reader.

Iron concentration measurement. Elemental iron concentrations in total brain, cortex, cerebellum, and hippocampus from the same P90 mice used for hematocrit measurement were determined by atomic absorptiometry as described elsewhere (11,20). The number of mice ranged from 4 to 14 per group. Samples were pooled from multiple mice to achieve sufficient tissue for evaluation of regional brain areas and structures. Values were expressed as μmol (of iron)/g dry weight.

Modified Perl's iron staining. Brain sections from P25 *Slc11a2*$^{hipp/hipp}$ ($n = 4$) and *Slc11a2*$^{WT/WT}$ ($n = 4$) mice (not used in other experiments) were stained for iron with a modification of the Perl's iron stain, as described previously (21) (22) (Supplemental Methods).

Tissue dissection and RNA collection. Male mice (not used in other experiments) at P5, P10, P15, P20, P25, P45, and P90 were killed by an intraperitoneal injection of Beuthanasia (10 mg/kg). Brains were removed from the cranium and bisected. The hippocampus was dissected and flash-frozen in liquid nitrogen. Total RNA was isolated using an RNA-isolation kit (Stratagene) and concentrations were measured by absorbance at 260 nm ($A_{260/280}$) using a NanoDrop ND-1000 (NanoDrop Technologies). In trained mice, hippocampal RNA was isolated as described above immediately after the last probe trial in the Morris water maze (MWM).

Quantitative real-time PCR. Messenger RNA levels were measured for 18 transcripts from P5 to P45–90 by real-time, quantitative PCR (qPCR) (Taqman) (**Supplemental Table 1**). Ten mRNA transcripts were used to assess iron metabolism, the neurometabalome, and dendritic structure (15,21,23–26). Six transcripts indexed pathophysiologic processes, including hypoxia, stress, and altered divalent metal metabolism that confound brain IDA models (23,27–33). RT was carried out using SuperScript III (Invitrogen) and random hexamer probes and 4 μg of total RNA was used to generate cDNAs (Supplemental Methods).

In vivo ^{1}H NMR spectroscopy. P90 *Slc11a2*$^{hipp/hipp}$ mice ($n = 6$) and *Slc11a2*$^{WT/WT}$ mice ($n = 6$), not used in other experiments, were examined with in vivo ^{1}H NMR spectroscopy at 9.4Tesla as previously described (34–39) (Supplemental Methods). All experiments were performed on a 9.4 T/31 cm magnet (Magnex Scientific) equipped with an 11-cm gradient coil insert (300 mT/m, 500 μs) and strong 2nd-order shim coils (Resonance Research). The magnet was interfaced to a Varian INOVA console (Varian). A quadrature surface radio frequency coil with 2 geometrically decoupled single-turn coils (14-mm diameter) was used for both RF transmission and reception. The position of the volume of interest (VOI) was selected based on multi-slice rapid acquisition relaxation-enhanced MRI. VOI were centered in the left dorsal hippocampus. The size of the VOI (5–6 μL) was adjusted to fit the anatomical structure of the hippocampus and to minimize partial volume effects (excluding cerebral cortex and ventricles). Metabolite concentrations were analyzed using the linear combination model (36).

Dendrite morphometry in hippocampal area Ammon's Horn 1. Morphometry studies were conducted on P45 as described previously (20). Cornus Ammon 1 (CA1; area 1 of Ammon's Horn in hippocampus) was assessed medially and laterally as described previously (15). Measurements were made of the length of the initial segment of the apical dendrite, defined as the segment extending from the pyramidal cell soma to the first proximal lateral branching point (20,40). Only dendrites visibly connected to cell soma were measured.

MWM. Two versions of the MWM were used in P90 mice. The first method utilized a moving platform that permitted a daily assessment of spatial memory (41); a visually cued version was used to test motivation and the capacity to swim. This version of the MWM was too difficult for the mice with hippocampal ID to learn. Thus, we used a 2nd, easier version of the MWM that utilized a fixed hidden platform that serially decreased in size (and thus increased in difficulty) over the training day to help the mice maintain a motivation to swim. For detailed behavioral methods, see Supplemental Methods.

Statistical analysis. For statistical comparisons between data from *Slc11a2*$^{hipp/hipp}$ and *Slc11a2*$^{WT/WT}$ mice in hematocrit, iron content, ^{1}H MRS, and dendrite morphometric studies, significance was determined using unpaired, 2-tailed Student's *t* tests.

Two-way ANOVA was performed with Cre status ($df = 1$), postnatal age ($df = 6$), and their interaction ($df = 6$) as fixed factors to determine

the effects of hippocampal-specific knockout of *Slc11a2* and postnatal age on qPCR determined mRNA expression. Bonferroni corrected post hoc *t* tests were performed for each fixed factor.

Mixed-model ANOVA (with repeated measures for day of training) was performed with Cre status ($df = 1$), day of training (MWM1, $df = 2$; MWM2, $df = 5$), and their interaction as fixed factors (MWM1, $df = 2$; MWM2, $df = 5$) to determine the effects of hippocampal specific knockout of *Slc11a2* and training on measures of MWM performance. Bonferroni corrected post hoc *t* tests were performed for each to compare for significant differences in memory performance on each day.

Two-way ANOVA was performed with Cre status ($df = 1$), MWM version ($df = 2$), and their interaction ($df = 2$) as fixed factors, to determine the effects of hippocampal specific knockout of *Slc11a2* and training on qPCR determined mRNA expression. Bonferroni corrected post hoc *t* tests were performed for each fixed factor. We made 3 a priori comparisons using unpaired 2-tailed Student's *t* tests: *1*) altered gene expression in trained versus untrained $Slc11a2^{WT/WT}$ mice after the difficult MWM (hard version); *2*) altered gene expression in $Slc11a2^{hipp/hipp}$ and $Slc11a2^{WT/WT}$ mice after the easier MWM version (enabling version); and *3*) altered gene expression in trained (easier MWM version) compared with untrained $Slc11a2^{hipp/hipp}$ mice.

Results

The hematocrits of the adult $Slc11a2^{hipp/hipp}$ (0.48 ± 0.01) and $Slc11a2^{WT/WT}$ mice (0.48 ± 0.01) were normal and did not different from each other. The hippocampal iron concentration was reduced by 42% ($P < 0.05$) in adult $Slc11a2^{hipp/hipp}$ mice compared with the wild type without reduction of whole brain, cerebellar, or cortical iron concentrations (**Fig. 1**). P25 $Slc11a2^{hipp/hipp}$ mice had less staining in all hippocampal subfields, including CA1 pyramidal neurons compared with $Slc11a2^{WT/WT}$ mice (**Fig. 2**; **Supplemental Fig. 1**).

Ten mRNA transcripts relevant to iron metabolism, neurometabolome, and dendritic structure (15,21,23–26) were different in $Slc11a2^{hipp/hipp}$ mice compared with $Slc11a2^{WT/WT}$ mice across all ages tested (Supplemental Table 1; **Fig. 3**; **Supplemental Fig. 2**). ANOVA statistics (Factor, F-statistic, *P*-value) for each comparison are listed in each figure legend. These included significantly lower *Slc11a2* mRNA levels in $Slc11a2^{hipp/hipp}$ mice with a probe designed for the region of deletion by Cre and a higher level of *TfRc* mRNA. Gene expression for *Aco1* iron responsive protein-1; (IRP-1) and *Ireb2* iron responsive protein-2; (IRP-2) and the 6 mRNA transcripts (*Adarb1*, *Ldha*, *Sod1*, *Sod2*, *Dio2*, and *Nr3c1*) that served as markers of pathophysiological processes to confound brain IDA models (23,27–33) did not differ between $Slc11a2^{WT/WT}$ and $Slc11a2^{hipp/hipp}$ mice.

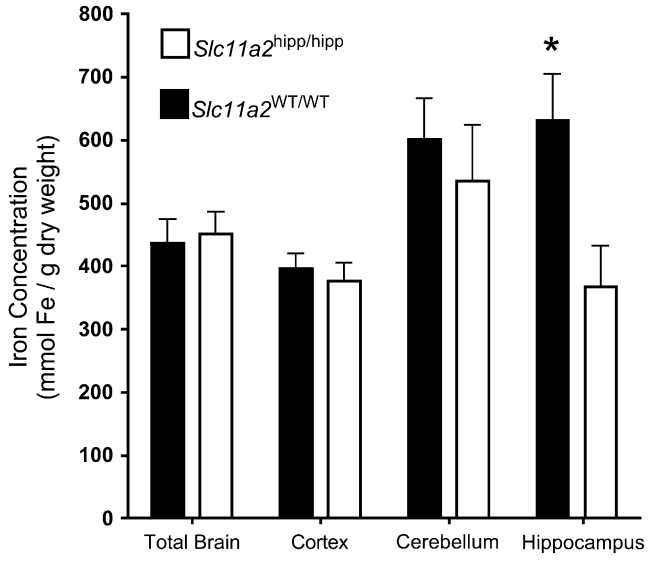

FIGURE 1 Regional iron concentrations in brains of $Slc11a2^{WT/WT}$ and $Slc11a2^{hipp/hipp}$ mice. Values are means ± SEM [$Slc11a2^{WT/WT}$: $n = 9$ total brains, 14 cortices, 13 cerebellum pools (4 cerebella/pool), 6 hippocampus pools (14 hippocampi/pool); $Slc11a2^{hipp/hipp}$: $n = 4$ total brains, 11 cortices, 7 cerebellum pools (4 cerebella/pool), 4 hippocampus pools (8 hippocampi/pool)]. *Different from $Slc11a2^{hipp/hipp}$, $P < 0.05$.

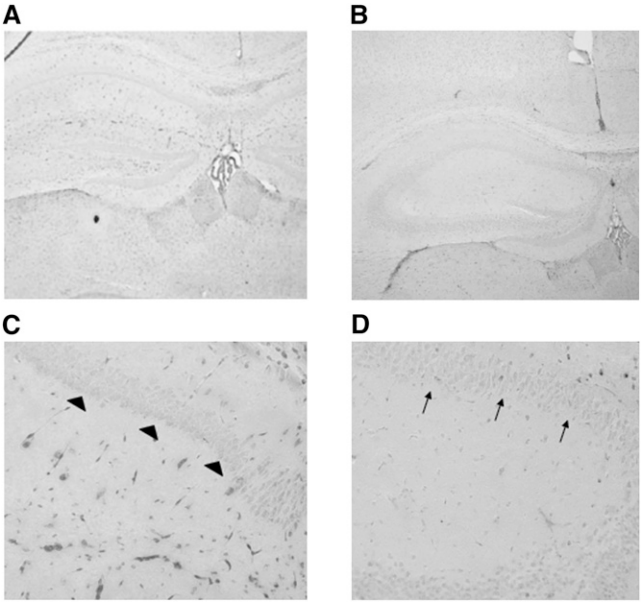

FIGURE 2 Perl's staining in hippocampus at P25 in $Slc11a2^{WT/WT}$ ($n = 4$) (*A,C*) and $Slc11a2^{hipp/hipp}$ (*B,D*) ($n = 4$) mice. Photomicrographs are at 100× (*A,B*) and 200× (*C,D*). Hippocampal area CA1 pyramidal neuronal soma in $Slc11a2^{hipp/hipp}$ mice show less staining (arrows) than $Slc11a2^{WT/WT}$ mice (arrowheads), whereas nonpyramidal cells localized between the hippocampal CA subfields and dentate gyrus retain positivity.

Among the 17 neurometabolites that could be reliably quantified by MRS in the hippocampus (**Supplemental Fig. 3**), phosphocreatine concentrations were 10% lower ($P < 0.01$) and lactate concentrations were 38% lower ($P < 0.01$) in $Slc11a2^{hipp/hipp}$ mice than in $Slc11a2^{WT/WT}$ controls (**Fig. 4**). The sum of glutamine (Gln) and glutamate (Glu) concentrations and the phosphocreatine:creatine ratio, which is directly related to cellular energy status $[ATP]/[ADP]_{free}$ (42,43), were decreased in $Slc11a2^{hipp/hipp}$ mice by 11% ($P < 0.05$) (**Supplemental Fig. 4**) and 13% ($P < 0.05$) (Fig. 4), respectively.

$Slc11a2^{hipp/hipp}$ mice had 20% shorter dendritic main shaft lengths (90 ± 4 μm) and disorganized branching patterns in area CA1 of hippocampus compared with $Slc11a2^{WT/WT}$ mice (113 ± 3 μm) at P45 ($P < 0.001$) (**Fig. 5**).

On the more difficult version of the MWM, $Slc11a2^{WT/WT}$ mice reached the criterion of spending 50% of their time searching in the target quadrant on d 3 of the probe trials ($P < 0.01$). $Slc11a2^{hipp/hipp}$ mice performed no better than chance and did not improve over time (**Fig. 6***A*). $Slc11a2^{hipp/hipp}$ mice had longer mean escape latencies and spent significantly less time in the target quadrant during training (Fig. 6*B*,*C*). During training, $Slc11a2^{hipp/hipp}$ mice appeared to have more bouts of immobility, confirmed by progressively slower mean swim velocities over the training days and more inactive time (Figs. 6*D*,*E*). There were no differences between groups in mean escape latency in

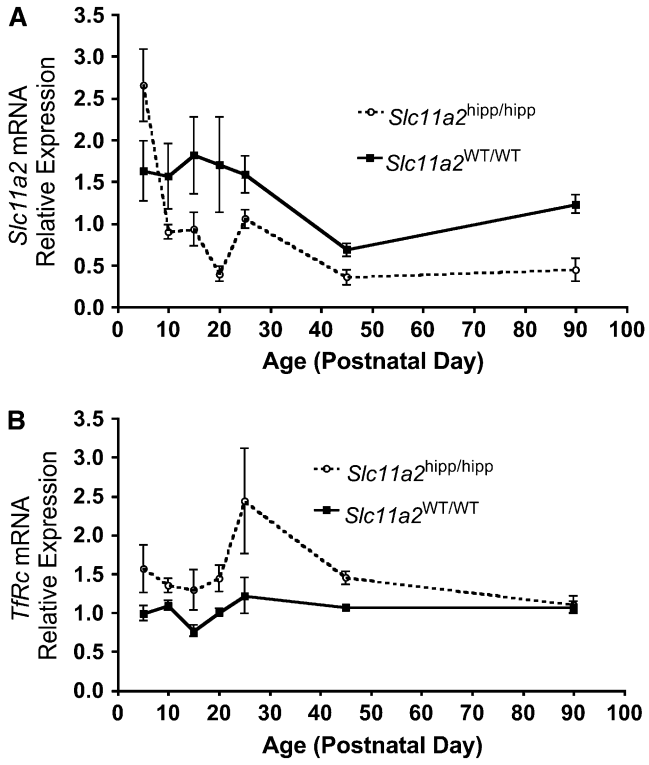

FIGURE 3 Hippocampal gene expression of *Slc11a2* exon 7 (*A*) and TfRc (*B*) in *Slc11a2*$^{WT/WT}$ and *Slc11a2*$^{hipp/hipp}$ mice from P5 to P90. Values are means ± SEM, $n = 3$–5. Significant effects ($P < 0.05$): *A*, Cre status, Age, Cre status × Age ; *B*, Cre status, Age.

the visual cued task, a control for procedural memory, sensorimotor function, motivation, and capacity to swim (data not shown).

In the easier 2nd version of the MWM, *Slc11a2*$^{WT/WT}$ mice again reached criterion on the probe trial after d 3 of training (**Supplemental Fig. 5**). *Slc11a2*$^{hipp/hipp}$ mice did not reach criterion by d 3 but, unlike their performance on the difficult version of the MWM, showed progressive improvement and met the criterion on the probe trial after d 4 of training. They swam at similar velocities, did not exhibit more floating behavior, spent similar amounts of time in the target quadrant, and had equal mean escape latencies during training as the *Slc11a2*$^{WT/WT}$ mice (Supplemental Fig. 5; data not shown). MWM1 and MWM2 ANOVA statistics (Factor, F-statistic, *P*-value) for each comparison are listed in each figure legend.

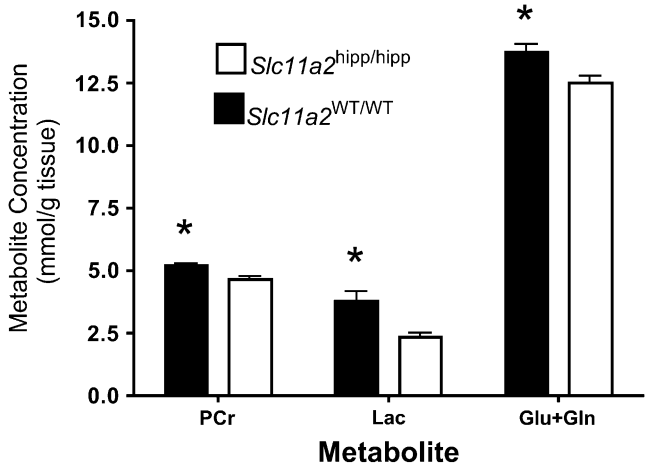

FIGURE 4 Hippocampus metabolite concentrations of *Slc11a2*$^{hipp/hipp}$ and *Slc11a2*$^{WT/WT}$ mice at P90. Values are means ± SEM, $n = 6$. *Different from *Slc11a2*$^{hipp/hipp}$, $P < 0.05$. Lac, lactate; PCr, phosphocreatine.

Spatial memory training induces gene expression in subfields of the hippocampus (44). Expression of 4 genes regulating iron metabolism and 2 regulating synaptic plasticity was altered based on Cre status or the interaction between Cre status and MWM version. Training on the harder version of the MWM induced upregulation of *Slc11a2*, *Tfrc*, *Aco1*, *Ireb2*, *Grin2b*, and *Camk2a* in *Slc11a2*$^{WT/WT}$ mice compared with the untrained condition. The easier version of the MWM elicited greater *Aco1* and *Camk2a* expression in trained compared with untrained *Slc11a2*^{hipphipp} mice. *Tfrc*, *Aco1*, *Ireb2*, *Grin2b*, and *Camk2a* expression was greater in *Slc11a2*^{hipphipp} mice trained on the easier MWM compared with *Slc11a2*$^{WT/WT}$ (**Fig. 7**). ANOVA statistics (Factor, F-statistic, *P*-value) for each comparison are listed in each figure legend.

Discussion

Iron is essential for life and whole-body knockout of the *Slc11a2* gene results in death in the first week of postnatal life (17). The role of iron in the developing brain has been of interest for over 25 y. Many of the studies on the subject fall into 2 categories: those that propose mechanisms of the generation and maintenance of iron homeostasis in the developing brain and those that investigate the consequences of iron dysregulation to that developing organ. Our model is of potential relevance for both. *Slc11a2* and its encoded protein DMT-1 are essential for iron uptake by hippocampal neurons. Deleting the gene in a timed, tissue-specific manner causes abnormal hippocampal neuronal development, energy metabolism, and neuronal structure. The results suggest that the neurocognitive findings in previous models using more global dietary or whole-animal mutant models of IDA were indeed due to the lack of hippocampal neuronal iron and occur independently of many of the potential coexisting confounders of those models.

Previous studies have identified processes that may explain how ID early in life leads to abnormal cognitive function. These include characterization of pathophysiological processes (e.g. hypoxia, cortisol activation, dysregulation of homeostasis of other micronutrients) and developmental processes (e.g. proliferation, cell death, differentiation). The studies have identified specific brain regions that are affected (e.g. hypothalamus-pituitary-adrenal axis, striatum, hippocampus), cell type-specific effects of ID, and particular iron-dependent biochemical reactions (e.g. oxidative phosphorylation, dopamine production, fatty acid metabolism, nucleotide synthesis) (45). Many of these are highly linked and coordinated, making it difficult to investigate the specific effect of iron on neuronal development and function in an in vivo model. The ability to eliminate DMT-1-mediated neuronal iron uptake during the postnatal hippocampal growth spurt allows for such an assessment.

We found significant differences in 10 mRNA transcripts that are relevant to the neurometabolomic, structural, and behavioral phenotypes we characterized in *Slc11a2*$^{hipp/hipp}$ mice. These include an expected decrease in *Slc11a2* mRNA in *Slc11a2*$^{hipp/hipp}$ mice compared with *Slc11a2*$^{WT/WT}$ littermates, with a probe designed for the region of deletion by Cre, and a significant increase in *TfRc* mRNA, which is upregulated in IDA (15,23), further confirming that our model induces hippocampal

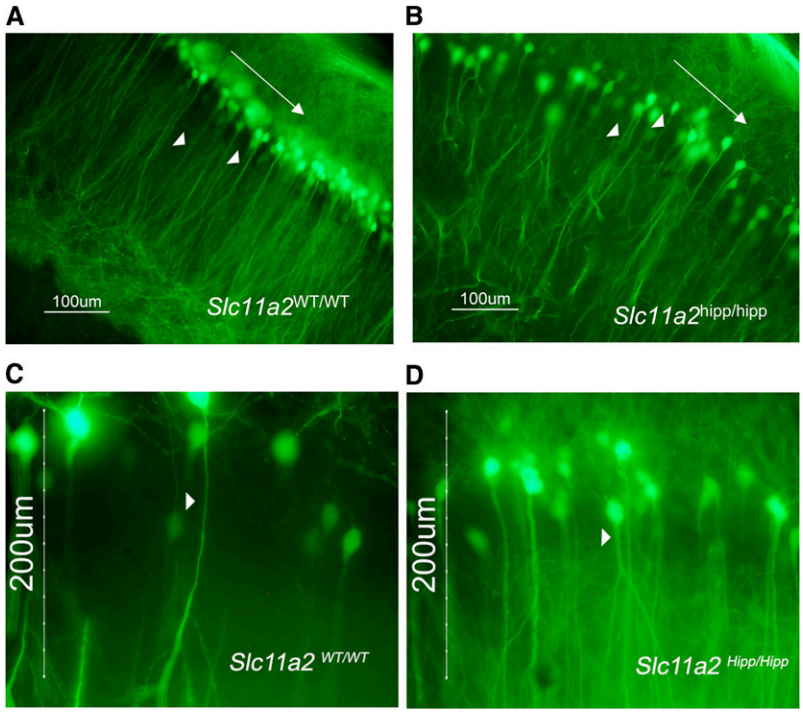

FIGURE 5 Visualization of pyramidal apical dendrite main shaft lengths in area CA1 of hippocampus of P45 *Slc11a2*$^{WT/WT}$ ($n = 9$) (*A,C*) and *Slc11a2*$^{hipp/hipp}$ ($n = 4$) (*B,D*) mice. Cell bodies are oriented longitudinally across the upper right of each panel, directionally denoted by the arrow. Apical dendrites in *Slc11a2*$^{WT/WT}$ mice and *Slc11a2*$^{hipp/hipp}$ mice are marked with arrowheads. Magnification at × 200 (*A,B*) and × 400 (*C,D*).

ID. Levels of *TfRc* mRNA returned to normal levels at P90, suggesting a lower iron demand in the P90 than in the P25 hippocampus. We observed significant upregulation of *Rasd1*, which has been shown to couple glutamate receptor activation to Slc11a2-mediated iron uptake in neurons (25). We also observed significant differences in developmental expression of Grin2a and Nos1, but not Grin2b, which are also part of the neuronal activity-dependent iron uptake mechanism (25). Significant differences in *Ckb* (creatine kinase, brain) and *Slc2a3* (neuronal glucose transporter Glut-3) were observed in *Slc11a2*$^{hipp/hipp}$ mice compared with *Slc11a2*$^{WT/WT}$ littermates, consistent with the decreased energy metabolism we characterized with MRS. We demonstrated significant differences in *Camk2a* and *Dlg4* (PSD-95), 2 genes that are imperative for normal dendrite development (24,26) and are also affected in an IDA model (23).

Slc11a2$^{hipp/hipp}$ mice and *Slc11a2*$^{WT/WT}$ littermates did not differ in the 6 mRNA transcripts that we used as markers of pathophysiological processes that confound brain IDA models. These included *Adarb1*, which is downregulated in hippocampal pyramidal neurons during hypoxia (30), and *Ldha*, a lactate dehydrogenase gene induced by hypoxia (27). DMT-1 has been

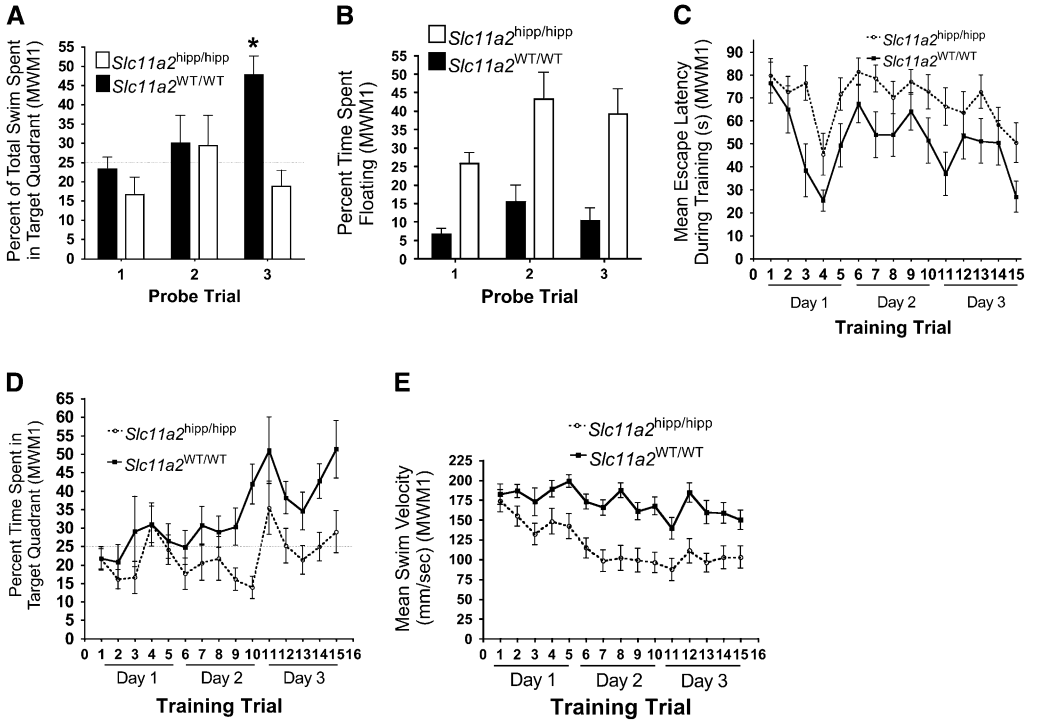

FIGURE 6 Spatial navigation memory in 3-mo-old *Slc11a2*$^{hipp/hipp}$ ($n = 15$) and *Slc11a2*$^{WT/WT}$ ($n = 12$) mice in the standard MWM (version 1). Values are means ± SEM. (*A*) Percent of total swim time spent in target quadrant on probe trials after each day of training. Significant effects ($P < 0.05$): Cre status, Training, Cre status × Training. (*B*) Percent time spent floating during probe trials. Significant effects ($P < 0.05$): Cre status, Training. (*C*) Mean escape latencies by trial across 3 training days. Significant effects ($P < 0.05$): Cre status, Training. (*D*) Percent time spent in target quadrant by trial across 3 training days. Significant effects ($P < 0.05$): Cre status, Training, Cre status × Training. (*E*) Mean swim velocity by trial across 3 training days. Significant effects ($P < 0.05$): Cre status, Training, Cre status × Training

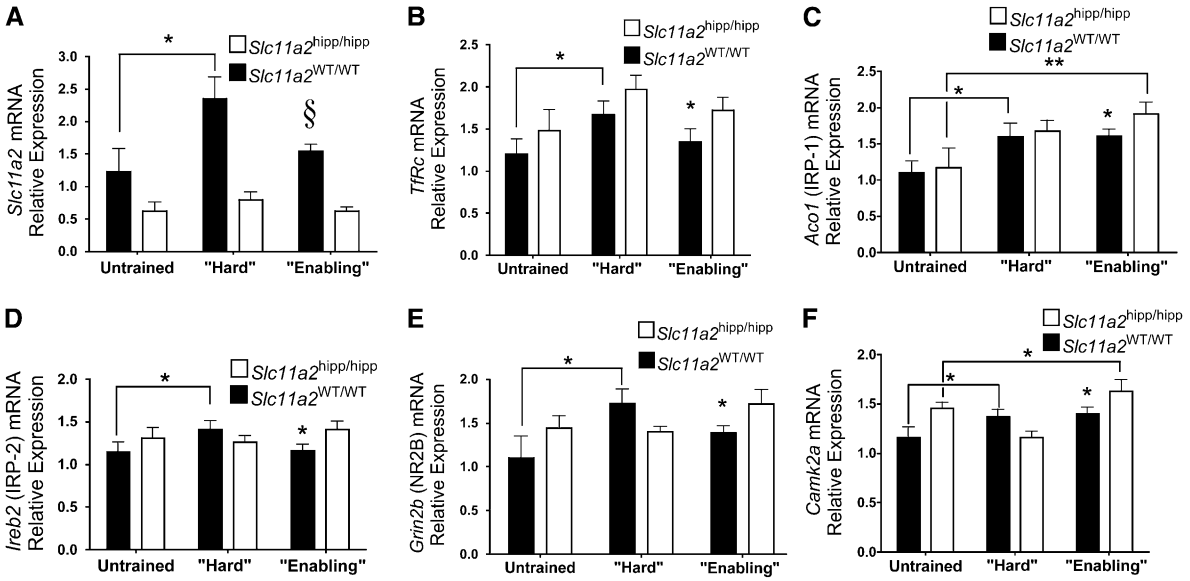

FIGURE 7 Gene expression in untrained, trained on hard MWM version 1, and trained on easier MWM version 2 *Slc11a2*$^{WT/WT}$ and *Slc11a2*$^{hipp/hipp}$ mice on P 90, quantified by qPCR. In each panel, the Y-axis represents units of relative mRNA expression with a value of 1.0 set for untrained *Slc11a2*$^{WT/WT}$ mice. Values are means ± SEM, $n = 7$–10 or 4 (untrained). Asterisks indicate that the designated groups differ: $*P < 0.05$; $**P < 0.01$ (unpaired 2-tailed Student's *t* tests). Significant effects in the 2-way ANOVA were: (*A*) *Slc11a2*; Cre status, MWM version, Cre status × MWM version; (*B*) Tfrc; Cre status, MWM version; (*C*) Aco1; MWM version; (*D*) *Ireb2*; Cre status, MWM version; (*E*) Grin2b; Cre status × MWM version; (*F*) Camk2a; MWM version, Cre status × MWM version.

shown to transport several other divalent cations both in vitro (46,47) and in vivo (48). Dietary IDA models alter brain levels of copper and manganese (49,50). The lack of upregulation of *Sod1*, a cytosolic copper-zinc superoxide dismutase gene that is upregulated in the presence of cadmium, copper, and zinc (33), and *Sod2*, a mitochondrial superoxide dismutase gene that is upregulated in the presence of manganese (31), suggests that dysregulation of noniron metal homeostasis in brain or hippocampus of *Slc11a2*$^{hipp/hipp}$ mice was unlikely. However, definitive measurements of copper, zinc, and manganese levels in the hippocampus of this mouse have not yet been performed. *Dio2*, a gene encoding the enzyme iodothyronine deiodinase type II, which activates thyroid hormone and is upregulated in IDA (23), was not altered in *Slc11a2*$^{hipp/hipp}$ mice compared with *Slc11a2*$^{WT/WT}$ littermates. Stress and glucocorticoid activity alter dendrite morphology of cells in the hippocampus in rodents (28,32,51,52). However, levels of *Nr3c1*, the gene encoding glucocorticoid receptor-1, did not differ in *Slc11a2*$^{hipp/hipp}$ and *Slc11a2*$^{WT/WT}$ mice.

Nonanemic ID in the *Slc11a2*$^{hipp/hipp}$ mouse altered glutamate balance and energy metabolism compared with *Slc11a2*$^{WT/WT}$ littermates. This is in contrast to IDA in the rat hippocampus, where changes in additional metabolites, such as markers of myelination (phosphorylcholine, phosphorylethanolamine, *myo*-inositol), GABAergic neurotransmission, and neuronal number (*N*-acetylaspartate) were found (37). These broader effects in the dietary model might have been due to the secondary effects of IDA rather than direct effects of ID. Our results are consistent with studies linking dietary ID after weaning with decreased brain glutamate concentrations (53,54). Iron levels regulate central nervous system glutamate formation and secretion via the iron-dependent enzyme cytosolic aconitase (IRP-1) in retinal pigment epithelial cells (55).

Normal glutamate and energy metabolism are critical for dendrite morphogenesis and synapse formation occurring between P15 and P25 (40,56). Iron import into the rat hippocampus is greatest immediately preceding the hippocampal growth spurt (prior to P15) and is characterized by the rapid appearance of iron transport and iron regulatory proteins (57,58). The shafts and spines of apical dendrites of CA1 pyramidal neurons are highly metabolic areas characterized by rapid local iron transmembrane cycling via TfR1 (59,60,61). The abnormal morphology found in *Slc11a2*$^{hipp/hipp}$ mice compared with *Slc11a2*$^{WT/WT}$ littermates suggests that this process was perturbed by the lack of neuronal iron uptake and could underlie the behavioral abnormalities. Although the alterations in energy metabolism did not appear to cause neuronal starvation and cell death, the cells may well have been in a state of energy conservation with limited ability to support growth during a critical period of dendritic differentiation.

The hippocampus has been implicated in several aspects of memory function, including acquisition, retrieval, and strategy switching (62,63). We attributed the abnormalities in spatial navigation memory performance in *Slc11a2*$^{hipp/hipp}$ mice to be dependent on the integrity of hippocampus and related to the structural and neurochemical changes we have demonstrated there. The results of the first spatial memory experiment, in which the hidden platform was moved between training trials within the target quadrant, could be explained by the *Slc11a2*$^{hipp/hipp}$ mice responding to the difficulty of the task with behavioral despair or learned helplessness, as in a Porsolt forced swim task (64). The results of the 2nd MWM experiment showed that the induction of bouts of immobility can be avoided when the task is made easier. Yet, the slower rate of learning and the later day the mice reached criterion in the probe test suggested that learning and memory systems were adversely affected in *Slc11a2*$^{hipp/hipp}$ mice compared with *Slc11a2*$^{WT/WT}$ littermates.

This is the first study, to our knowledge, confirming that spatial memory training induces experience-dependent iron uptake in hippocampus in wild-type mice and that hippocampal neuron-specific deletion of *Slc11a2* alters experience-dependent

gene expression related to iron uptake and synaptic plasticity. The 2 versions of the MWM allowed us to assess whether iron uptake by DMT-1 is required for learning in the more difficult version. When we enabled learning in the 2nd MWM version, *Slc11a2*-deficient hippocampal neurons responded with increased expression of both iron uptake and regulatory mRNAs and 2 markers of neuronal plasticity (*Grin2b* and *Camk2a*), and *Aco1* in *Slc11a2*$^{hipp/hipp}$ mice compared with *Slc11a2*$^{WT/WT}$ littermates, despite iron depletion. These results suggested that iron is not essential for learning and plasticity but that proper iron balance greatly facilitates it. In light of this, the mechanism of activity-dependent iron uptake proposed by Cheah et al. (25) may, under normal physiologic conditions, be a mechanism to promote proper iron balance required for normal memory formation in the hippocampus.

Our model is particularly relevant to understanding abnormal cognitive function due to fetal/neonatal ID in newborn humans. Hippocampus-based auditory recognition memory is compromised in nonanemic ID infants of diabetic mothers (3), who also showed deficits in memory of multi-step event sequences compared with typically developing controls at 1 y of age (2). One implication of the behavioral results in *Slc11a2*$^{hipp/hipp}$ mice for clinical treatment is that interventions that facilitate learning may improve cognitive outcomes in formerly ID children.

The model we present here will be useful in studying many aspects of iron in neurobiology, neurodevelopment, behavior, and experience-dependent plasticity such as cell death, neurogenesis, and synaptogenesis. It also offers an opportunity to study intracellular distribution of iron and how iron homeostasis is sensed and maintained among the many neural cell subtypes residing in hippocampus.

Acknowledgments

We thank Raghu Rao for encouragement and facilitation of MRS experiments, Mu Sun for training ESC in use of behavioral apparatus and software, and Roger H. Carlson for his help with the MWM apparatus and help running the MWM tests.

Literature Cited

1. Lozoff B, Georgieff MK. Iron deficiency and brain development. Semin Pediatr Neurol. 2006;13:158–65.
2. DeBoer T, Wewerka S, Bauer PJ, Georgieff MK, Nelson CA. Explicit memory performance in infants of diabetic mothers at 1 year of age. Dev Med Child Neurol. 2005;47:525–31.
3. Siddappa AM, Georgieff MK, Wewerka S, Worwa C, Nelson CA, Deregnier RA. Iron deficiency alters auditory recognition memory in newborn infants of diabetic mothers. Pediatr Res. 2004;55:1034–41.
4. Felt BT, Beard JL, Schallert T, Shao J, Aldridge JW, Connor JR, Georgieff MK, Lozoff B. Persistent neurochemical and behavioral abnormalities in adulthood despite early iron supplementation for perinatal iron deficiency anemia in rats. Behav Brain Res. 2006;171:261–70.
5. Felt BT, Lozoff B. Brain iron and behavior of rats are not normalized by treatment of iron deficiency anemia during early development. J Nutr. 1996;126:693–701.
6. McEchron MD, Alexander DN, Gilmartin MR, Paronish MD. Perinatal nutritional iron deficiency impairs hippocampus-dependent trace eyeblink conditioning in rats. Dev Neurosci. 2008;30:243–54.
7. McEchron MD, Cheng AY, Liu H, Connor JR, Gilmartin MR. Perinatal nutritional iron deficiency permanently impairs hippocampus-dependent trace fear conditioning in rats. Nutr Neurosci. 2005;8:195–206.
8. Schmidt AT, Waldow KJ, Grove WM, Salinas JA, Georgieff MK. Dissociating the long-term effects of fetal/neonatal iron deficiency on three types of learning in the rat. Behav Neurosci. 2007;121:475–82.
9. Lozoff B, Beard J, Connor J, Barbara F, Georgieff M, Schallert T. Long-lasting neural and behavioral effects of iron deficiency in infancy. Nutr Rev. 2006;64:S34–43.
10. Lozoff B, Jimenez E, Smith JB. Double burden of iron deficiency in infancy and low socioeconomic status: a longitudinal analysis of cognitive test scores to age 19 years. Arch Pediatr Adolesc Med. 2006;160:1108–13.
11. Jorgenson LA, Sun M, O'Connor M, Georgieff MK. Fetal iron deficiency disrupts the maturation of synaptic function and efficacy in area CA1 of the developing rat hippocampus. Hippocampus. 2005;15:1094–102.
12. Moos T, Morgan EH. Transferrin and transferrin receptor function in brain barrier systems. Cell Mol Neurobiol. 2000;20:77–95.
13. Roberts R, Sandra A, Siek GC, Lucas JJ, Fine RE. Studies of the mechanism of iron transport across the blood-brain barrier. Ann Neurol. 1992;32 Suppl:S43–50.
14. Moos T, Rosengren Nielsen T, Skjorringe T, Morgan EH. Iron trafficking inside the brain. J Neurochem. 2007;103:1730–40.
15. Siddappa AJ, Rao RB, Wobken JD, Casperson K, Leibold EA, Connor JR, Georgieff MK. Iron deficiency alters iron regulatory protein and iron transport protein expression in the perinatal rat brain. Pediatr Res. 2003;53:800–7.
16. Hemar A, Olivo JC, Williamson E, Saffrich R, Dotti CG. Dendroaxonal transcytosis of transferrin in cultured hippocampal and sympathetic neurons. J Neurosci. 1997;17:9026–34.
17. Gunshin H, Fujiwara Y, Custodio AO, Direnzo C, Robine S, Andrews NC. Slc11a2 is required for intestinal iron absorption and erythropoiesis but dispensable in placenta and liver. J Clin Invest. 2005;115:1258–66.
18. Dragatsis I, Zeitlin S. CaMKIIalpha-Cre transgene expression and recombination patterns in the mouse brain. Genesis. 2000;26:133–5.
19. Feng G, Mellor RH, Bernstein M, Keller-Peck C, Nguyen QT, Wallace M, Nerbonne JM, Lichtman JW, Sanes JR. Imaging neuronal subsets in transgenic mice expressing multiple spectral variants of GFP. Neuron. 2000;28:41–51.
20. Jorgenson LA, Wobken JD, Georgieff MK. Perinatal iron deficiency alters apical dendritic growth in hippocampal CA1 pyramidal neurons. Dev Neurosci. 2003;25:412–20.
21. Benkovic SA, Connor JR. Ferritin, transferrin, and iron in selected regions of the adult and aged rat brain. J Comp Neurol. 1993;338:97–113.
22. de Deungria M, Rao R, Wobken JD, Luciana M, Nelson CA, Georgieff MK. Perinatal iron deficiency decreases cytochrome c oxidase (CytOx) activity in selected regions of neonatal rat brain. Pediatr Res. 2000;48:169–76.
23. Carlson ES, Stead JD, Neal CR, Petryk A, Georgieff MK. Perinatal iron deficiency results in altered developmental expression of genes mediating energy metabolism and neuronal morphogenesis in hippocampus. Hippocampus. 2007;17:679–91.
24. Charych EI, Akum BF, Goldberg JS, Jornsten RJ, Rongo C, Zheng JQ, Firestein BL. Activity-independent regulation of dendrite patterning by postsynaptic density protein PSD-95. J Neurosci. 2006;26:10164–76.
25. Cheah JH, Kim SF, Hester LD, Clancy KW, Patterson SE III, Papadopoulos V, Snyder SH. NMDA receptor-nitric oxide transmission mediates neuronal iron homeostasis via the GTPase Dexras1. Neuron. 2006;51:431–40.
26. Gaudilliere B, Konishi Y, de la Iglesia N, Yao G, Bonni AA. CaMKII-NeuroD signaling pathway specifies dendritic morphogenesis. Neuron. 2004;41:229–41.
27. Firth JD, Ebert BL, Ratcliffe PJ. Hypoxic regulation of lactate dehydrogenase A. Interaction between hypoxia-inducible factor 1 and cAMP response elements. J Biol Chem. 1995;270:21021–7.
28. Hashimoto H, Marystone JF, Greenough WT, Bohn MC. Neonatal adrenalectomy alters dendritic branching of hippocampal granule cells. Exp Neurol. 1989;104:62–7.
29. Koibuchi N, Chin WW. Thyroid hormone action and brain development. Trends Endocrinol Metab. 2000;11:123–8.
30. Peng PL, Zhong X, Tu W, Soundarapandian MM, Molner P, Zhu D, Lau L, Liu S, Liu F, et al. ADAR2-dependent RNA editing of AMPA receptor subunit GluR2 determines vulnerability of neurons in forebrain ischemia. Neuron. 2006;49:719–33.

31. Thongphasuk J, Oberley LW, Oberley TD. Induction of superoxide dismutase and cytotoxicity by manganese in human breast cancer cells. Arch Biochem Biophys. 1999;365:317–27.
32. Watanabe Y, Gould E, McEwen BS. Stress induces atrophy of apical dendrites of hippocampal CA3 pyramidal neurons. Brain Res. 1992; 588:341–5.
33. Yoo HY, Chang MS, Rho HM. Heavy metal-mediated activation of the rat Cu/Zn superoxide dismutase gene via a metal-responsive element. Mol Gen Genet. 1999;262:310–3.
34. Gruetter R. Automatic, localized in vivo adjustment of all first- and second-order shim coils. Magn Reson Med. 1993;29:804–11.
35. Gruetter R, Tkac I. Field mapping without reference scan using asymmetric echo-planar techniques. Magn Reson Med. 2000;43:319–23.
36. Provencher SW. Estimation of metabolite concentrations from localized in vivo proton NMR spectra. Magn Reson Med. 1993;30:672–9.
37. Rao R, Tkac I, Townsend EL, Gruetter R, Georgieff MK. Perinatal iron deficiency alters the neurochemical profile of the developing rat hippocampus. J Nutr. 2003;133:3215–21.
38. Tkac I, Henry PG, Andersen P, Keene CD, Low WC, Gruetter R. Highly resolved in vivo 1H NMR spectroscopy of the mouse brain at 9.4 T. Magn Reson Med. 2004;52:478–84.
39. Tkac I, Starcuk Z, Choi IY, Gruetter R. In vivo 1H NMR spectroscopy of rat brain at 1 ms echo time. Magn Reson Med. 1999;41:649–56.
40. Pokorny J, Yamamoto T. Postnatal ontogenesis of hippocampal CA1 area in rats. I. Development of dendritic arborisation in pyramidal neurons. Brain Res Bull. 1981;7:113–20.
41. Choi SH, Woodlee MT, Hong JJ, Schallert T. A simple modification of the water maze test to enhance daily detection of spatial memory in rats and mice. J Neurosci Methods. 2006;156:182–93.
42. Erecinska M, Silver IA. ATP and brain function. J Cereb Blood Flow Metab. 1989;9:2–19.
43. Siesjo BK. Brain energy metabolism and catecholaminergic activity in hypoxia, hypercapnia and ischemia. J Neural Transm Suppl. 1978;17–22.
44. Vann SD, Brown MW, Erichsen JT, Aggleton JP. Fos imaging reveals differential patterns of hippocampal and parahippocampal subfield activation in rats in response to different spatial memory tests. J Neurosci. 2000;20:2711–8.
45. Beard JL, Wiesinger JA, Connor JR. Pre- and postweaning iron deficiency alters myelination in Sprague-Dawley rats. Dev Neurosci. 2003;25:308–15.
46. Gunshin H, Mackenzie B, Berger UV, Gunshin Y, Romero MF, Boron WF, Nussberger S, Gollan JL, Hediger MA. Cloning and characterization of a mammalian proton-coupled metal-ion transporter. Nature. 1997;388:482–8.
47. Garrick MD, Singleton ST, Vargas F, Kuo HC, Zhao L, Knopfel M, Davidson T, Costa M, Paradkar P, et al. DMT1: which metals does it transport? Biol Res. 2006;39:79–85.
48. Knopfel M, Zhao L, Garrick MD. Transport of divalent transition-metal ions is lost in small-intestinal tissue of b/b Belgrade rats. Biochemistry. 2005;44:3454–65.
49. Garcia SJ, Gellein K, Syversen T, Aschner M. Iron deficient and manganese supplemented diets alter metals and transporters in the developing rat brain. Toxicol Sci. 2007;95:205–14.
50. Crossgrove JS, Yokel RA. Manganese distribution across the blood-brain barrier III. The divalent metal transporter-1 is not the major mechanism mediating brain manganese uptake. Neurotoxicology. 2004;25:451–60.
51. Magarinos AM, McEwen BS. Stress-induced atrophy of apical dendrites of hippocampal CA3c neurons: involvement of glucocorticoid secretion and excitatory amino acid receptors. Neuroscience. 1995;69:89–98.
52. Magarinos AM, McEwen BS, Flugge G, Fuchs E. Chronic psychosocial stress causes apical dendritic atrophy of hippocampal CA3 pyramidal neurons in subordinate tree shrews. J Neurosci. 1996;16:3534–40.
53. Taneja V, Mishra K, Agarwal KN. Effect of early iron deficiency in rat on the gamma-aminobutyric acid shunt in brain. J Neurochem. 1986; 46:1670–4.
54. Shukla A, Agarwal KN, Shukla GS. Latent iron deficiency alters gamma-aminobutyric acid and glutamate metabolism in rat brain. Experientia. 1989;45:343–5.
55. McGahan MC, Harned J, Mukunnemkeril M, Goralska M, Fleisher L, Ferrell JB. Iron alters glutamate secretion by regulating cytosolic aconitase activity. Am J Physiol Cell Physiol. 2005;288:C1117–24.
56. Rihn LL, Claiborne BJ. Dendritic growth and regression in rat dentate granule cells during late postnatal development. Brain Res Dev Brain Res. 1990;54:115–24.
57. Taylor EM, Morgan EH. Developmental changes in transferrin and iron uptake by the brain in the rat. Brain Res Dev Brain Res. 1990;55:35–42.
58. Siddappa AJ, Rao RB, Wobken JD, Leibold EA, Connor JR, Georgieff MK. Developmental changes in the expression of iron regulatory proteins and iron transport proteins in the perinatal rat brain. J Neurosci Res. 2002;68:761–75.
59. Burack MA, Silverman MA, Banker G. The role of selective transport in neuronal protein sorting. Neuron. 2000;26:465–72.
60. Silverman MA, Kaech S, Jareb M, Burack MA, Vogt L, Sonderegger P, Banker G. Sorting and directed transport of membrane proteins during development of hippocampal neurons in culture. Proc Natl Acad Sci USA. 2001;98:7051–7.
61. Blanpied TA, Scott DB, Ehlers MD. Age-related regulation of dendritic endocytosis associated with altered clathrin dynamics. Neurobiol Aging. 2003;24:1095–104.
62. Day LB, Weisand M, Sutherland RJ, Schallert T. The hippocampus is not necessary for a place response but may be necessary for pliancy. Behav Neurosci. 1999;113:914–24.
63. Squire LR. Memory and the hippocampus: a synthesis from findings with rats, monkeys, and humans. Psychol Rev. 1992;99:195–231.
64. Porsolt RD, Le Pichon M, Jalfre M. Depression: a new animal model sensitive to antidepressant treatments. Nature. 1977;266:730–2.